

The one-electron Green's function of the half-filled Hubbard model on a triangular lattice

M.C. Refolio, J.M. López Sancho, and J. Rubio
Instituto de Matemáticas y Física Fundamental, CSIC
Serrano 113 bis, 28006 Madrid, Spain
e-mail: refolio@imaff.cfmac.csic.es
Fax: +34-(1)5854894

Abstract

The one-electron density of states for the half-filled Hubbard model on a triangular lattice is studied as a function of both temperature and Hubbard U using Quantum Monte Carlo. We find three regimes: (1) a strong-coupling Mott-Hubbard regime, characterized by a gap which persists even at high temperatures; (2) a weak-coupling paramagnetic regime, characterized by the absence of a pseudogap at any finite temperature; and (3) an intermediate-coupling (spiral) spin-density-wave regime, characterized by a pseudogap which appears when U is increased beyond a critical (temperature dependent) value. The behavior of the $\sqrt{3} \times \sqrt{3}$ adlayer structures on fourth-group semiconductor surfaces is briefly commented upon in the light of the above discussion.

Keywords Hubbard modeling. Semiconducting surfaces. Charge and spin density waves. Surface Mott insulators.

PACS: 73.20.At; 75.30.Fv; 75.30.Pd; 71.15.Mb

I. INTRODUCTION

As is well-known, the frustration effects associated with the triangular lattice often lead to non-trivial ground-state degeneracies as in the antiferromagnetic (AF) spin 1/2 Ising model [1,2]. The classical Heisenberg model on the two-dimensional (2D) triangular lattice with nearest-neighbor AF coupling and easy-axis exchange anisotropy is another example where frustration leads to a novel ground-state degeneracy. This system has attracted much attention especially since Anderson [3] suggested the possibility of a resonating-valence-bond ground state for the spin one-half case. Simply, the quantum liquid of randomly distributed spin-singlet pairs could be an efficient way to overcome the frustration of the Néel state in the triangular antiferromagnet. One more important source of interest in these lattices is the well-known diversity and richness of physical phenomena displayed by most transition metal compounds [4].

The experimental observation of low-temperature insulating phases in some $\sqrt{3}$ -adlayer structures on (111) Si and Ge surfaces has only fostered the interest in these 2D triangular lattices. Thus, whereas the $\sqrt{3}$ -overlayers of Sn and Pb on Ge(111) are both metallic at high

temperature, their corresponding low-temperature counterparts are either metallic, as in the case of Sn [5–7], or weakly insulating as in the case of Pb [8–10]. This latter system seems to go through some kind of reversible metallic to insulating transition whose precise nature is still controversial [11–13]. A charge-density wave (CDW) has been invoked in the case of Pb (but not in the case of Sn) as the driving force for the destabilization of the high-temperature phase, a conjecture not universally accepted at the time of writing. Related isoelectronic systems, on the other hand, like the $\sqrt{3} \times \sqrt{3}$ adlayer of Si on SiC(0001) [14], or of K on Si(111):B [15] show a clear insulating behavior with a large gap and no phase transitions. These systems have been studied theoretically both within the local-density (LDA) [5,16,17] and the Hartree-Fock [18,19] approximations. Quite recently [20] the LDA+U approach has been used to include strong on-site repulsions in SiC(0001).

In this paper we carry out a model study of the triangular lattice in order to explore some general questions any realistic theory should comply with. For instance understanding the temperature behavior of the one-electron density of states (DOS) is essential to the development of a complete picture of these metal-insulator transitions. Hence we report the results of a Quantum Monte Carlo (QMC) simulation of the half-filled Hubbard model on such a triangular lattice in the grand canonical ensemble. The one-electron Green’s function is studied as a function of both temperature and coupling constant (Hubbard U). As the temperature is lowered, a pseudogap develops in the one-electron DOS for intermediate values of U . This pseudogap is accompanied by two weak peaks in the spin structure factor which signal the formation of a spiral spin-density-wave (SDW). For lower U , no gap at all is found even for low temperatures, the system remaining always paramagnetic. For higher U , on the other hand, a well developed gap appears at any temperature, accompanied by a strong peak in the spin structure factor. The system is then brought into a state very similar to the ground state of the triangular antiferromagnet (the three-sublattice model). We emphasize that these are not distinct phases, but only different regimes with smooth transitions among them, as characterized by the behavior of the one-electron DOS. Since the presence or absence of a gap or pseudogap is of fundamental importance in determining the properties of a system, we believe that this type of characterization is useful and can be of help in understanding the electronic properties of the more complex adsorption systems referred to above.

The paper is organized as follows: Section II recalls some of the basic properties of the triangular lattice as well as the Hubbard model, in order to fix the notation. Sec III summarizes very briefly the Quantum Monte Carlo algorithm in the grand canonical ensemble. The resulting one-electron DOS and spin structure factor are displayed and discussed in Sec IV and, finally, the paper closes with some concluding remarks in Sec V

II. BASIC PROPERTIES OF THE TRIANGULAR LATTICE AND HAMILTONIAN

In the $\sqrt{3} \times \sqrt{3}$ R30° adlayer structures of Sn or Pb on Ge(111) at one third coverage, each adsorbate sits on top of a triangle of Ge atoms. With just one unpaired electron per adsorbate, the overlayer is half-filled and, therefore, metallic in the absence of electron-electron interactions. This overlayer can in turn be described as a 3×3 lattice of adsorbate triangles (the three-sublattice model) with three unpaired electrons per triangle and, therefore, again

metallic in the absence of interaction. The corresponding surface Brillouin zones (SBZ) are the large and small hexagon, respectively, in Fig 1. The adlayer $\sqrt{3} \times \sqrt{3}$ lattice has just one band in the large zone, ϵ_k^0 , which folds onto three bands in the small zone. Fig 2 shows these three bands, ϵ_k^0 , ϵ_k^+ , and ϵ_k^- , unfolded in the extended zone scheme in order to see the nesting properties. They are given by (t =hopping strength)

$$\epsilon_k^0 = 2t \cos kx + 4t \cos \frac{1}{2}k_x \cos \frac{\sqrt{3}}{2}k_y \quad (1)$$

$$\epsilon_k^\pm = -\frac{1}{2}\epsilon_k^0 \pm t\sqrt{3} \left(\sin k_x - 2 \sin \frac{1}{2}k_x \cos \frac{\sqrt{3}}{2}k_y \right) \quad (2)$$

It is easy to see that ϵ_k^\pm are just ϵ_k^0 for $k = (k_x \pm \frac{2\pi}{3}, k_y)$. These bands cross at the points M' and K' . The wavevector $K=(4\pi/3, 0)$ turns out to be a nesting vector with the band folding around the $M'=0.5 K$ point ($M'K \rightarrow M'\Gamma$, band ϵ_k^+). Likewise $KM \rightarrow \Gamma M'$ (band ϵ_k^-). Fig 3, finally, shows the resulting band along the small SBZ contour. Notice that the $M'K'$ direction is obtained by folding the MK' portion of ϵ_k^0 .

This is of no consequence for the interaction-free system at half filling since the Fermi surface is not anywhere close enough to either the large or the small SBZ boundaries. When the interaction is turned on, however, the nesting symmetry may come into play, although weakly, at the points M and M' , closest to the Fermi surface. We shall see that, even at half-filling, this is indeed the case for the spin structure factor when U is large enough.

In order to describe the interacting system, we adopt the Hubbard model, given by the standard Hamiltonian

$$H = t \sum_{\langle ij \rangle s} c_{is}^+ c_{js} - \mu \sum_{is} n_{is} + U \sum_i \left((n_{i\uparrow} - \frac{1}{2})(n_{i\downarrow} - \frac{1}{2}) \right) \quad (3)$$

where t is the hopping strength, U the on-site repulsion and μ the chemical potential. The single sums run over all the $N \times N$ adlayer atoms and the symbol $\langle \rangle$ means summation over nearest neighbors (nn). As usual, c_{is}^+ creates, while c_{is} destroys, an electron of spin s at site i with occupation number $n_{is} = c_{is}^+ c_{is}$. We take $t=0.055$ eV so as to start with a narrow adlayer bandwidth ($W=9t$) of around 0.5 eV at $U=0$. U is varied to cover different regimes of the triangular lattice and μ is adjusted so as to have always half filling. Recall that, unlike the case of bipartite lattices, $\mu = U/2$ does not necessarily correspond to half-filling since particle-hole symmetry does not hold in a triangular lattice.

This Hubbard model is now simulated by the QMC approach in the grand canonical ensemble as initially developed by Blankenbecler et al [21] and supplemented by a discrete lattice version of the Hubbard-Stratonovich transformation by Hirsch [22]. The whole approach has been explained at length by Hirsch [23] and White et al [24] and is briefly summarized in the following section.

III. QUANTUM MONTE CARLO ALGORITHM

In a grand canonical simulation [21–24] the imaginary time is discretized through the introduction of L time slices separated by an interval $\Delta\tau$ such that $\beta=\Delta\tau L$. The partition function is then written as

$$Z = \text{Tr} e^{-\beta H} = \text{Tr} e^{-\Delta\tau L H} \simeq \text{Tr} (e^{-\Delta\tau \hat{K}} e^{-\Delta\tau \hat{V}})^L, \quad (4)$$

where

$$\hat{K} = t \sum_{\langle ij \rangle} c_{is}^+ c_{js} - \mu \sum_{is} n_{is} = \sum_{\langle ijs \rangle} K_{ij} c_{is}^+ c_{js} \quad (5)$$

and

$$\hat{V} = U \sum_i \left(n_{\uparrow} - \frac{1}{2} \right) \left(n_{\downarrow} - \frac{1}{2} \right). \quad (6)$$

The last step in Eq(4) follows from the Trotter formula [25] which introduces systematic errors in the measured quantities of order $\Delta\tau^2$. One should therefore like to take $\Delta\tau$ as small as possible, although keeping the number of time slices not too large. This poses a serious limitation at low temperatures (large β).

A discrete Hubbard-Stratonovich (HS) transformation [22] is now performed for each on-site interaction term within any time slice.

$$e^{-\Delta\tau U (n_{i\uparrow} - \frac{1}{2})(n_{i\downarrow} - \frac{1}{2})} = \frac{1}{2} e^{-\Delta\tau U/4} \text{Tr}_{\sigma} e^{-\Delta\tau \lambda \sigma_{il} (n_{i\uparrow} - n_{i\downarrow})} \quad (7)$$

where a discrete, auxiliary Ising field $\sigma_{il} = \pm 1$ (l runs through the L time slices) has been introduced and $\cosh \lambda \Delta\tau = e^{U\Delta\tau/2}$. Tr_{σ} means summation over the NL Ising "spins" σ_{il} , which define the auxiliary Ising field through the lattice sites and time slices. Defining now $N \times N$ matrices $V(l)$ such that

$$V_{ij}(l) = \frac{1}{2} \delta_{ij} \lambda s_{ij}, \quad (8)$$

we can write

$$Z = \left(\frac{1}{2} e^{-\Delta\tau U/4} \right)^{NL} \text{Tr}_{\sigma} \text{Tr} \Pi_{s,l} D_l^s, \quad (9)$$

where

$$D_l^s = e^{-\Delta\tau \sum_{ijs} K_{ij} c_{is}^+ c_{js}} e^{-\Delta\tau \sum_{is} V_{ii}(l) \alpha_s n_{is}} \quad (10)$$

where $\alpha_s = \pm 1$ for $s = \uparrow \downarrow$ respectively. Notice carefully the difference between σ , Ising spin, and s , fermion spin.

The fermion degrees of freedom can be traced over [21,23] to yield

$$Z = \text{Tr}_{\sigma} \Pi_s \det 0_s [\sigma] \quad (11)$$

where $0_s [\sigma]$, the fermion matrix, is given by

$$0_s = I + B_l^s B_{l-1}^s \dots B_1^s \quad (12)$$

with

$$B_l^s = e^{-\Delta\tau K} e^{-\Delta\tau\alpha_s V(l)} \quad (13)$$

and I being the unity matrix. Therefore $\Pi_s \det 0_s$ plays the role of a Boltzmann weight for evaluating the average of any operator, $\langle A \rangle = \text{Tr} A e^{-\beta H} / \text{Tr} e^{-\beta H}$. The above steps must now be repeated for $\text{Tr} A e^{-\beta H}$. Thus for $A = c_{is} c_{js}^+$, the resulting expression is

$$\text{Tr} (c_{is} c_{js}^+ e^{-\beta H}) = \text{Tr}_\sigma (0_s^{-1})_{ij} \Pi_s \det 0_s [\sigma] \quad (14)$$

and hence an equal-time single particle Green's function $\langle c_{is} c_{js}^+ \rangle$ is obtained by averaging the corresponding matrix elements of the inverse of the fermion matrix 0_s . Time dependent Green's functions can also be calculated and involve slightly more complicated matrices [23]. For any HS field configuration, Wick's theorem for operator products applies and one can therefore easily calculate time-dependent correlation functions in terms of single-particle Green's functions for any given Ising configuration. These imaginary-time quantities are then to be analytically continued to real time and frequencies via the maximum-entropy method [26,27] which yields the corresponding spectral weight functions.

The heat-bath algorithm is used to sample the HS field subject to the Boltzmann weight given above. This sampling is normally accomplished by single spin-flips $\sigma_{il} \rightarrow -\sigma_{il}$, the corresponding weight-ratio being related to equal-time Green's function [21,24]. If the new configuration is accepted, the corresponding Green's functions is updated through simple operations [21,24]. Calculating the weight ratio requires N^2 operations, and therefore $N^3 L$ operations must be done for a sweep through the whole HS field. Normally two hundred warm-up sweeps and one thousand measurements separated by two sweeps were performed for each set of parameters. At low temperatures the algorithm becomes unstable due to the large number of time slices required in order to make $\Delta\tau$ small enough. The product of B matrices in Eq(12) is ill-conditioned and one has to resort to matrix factorization techniques [24].

IV. THE THREE COUPLING REGIMES

According to the Mermin-Wagner theorem [28], infinite-range magnetic order is forbidden in two dimensions at any $T \neq 0$. This is so because the Goldstone modes strongly disorder the system giving rise to a spin-spin correlation length which decays with temperature as $\xi(T) \sim \exp(A/T)$, where A is a constant. Thus no phase transitions of magnetic origin can take place in an infinite system except, perhaps, at $T=0$. Other kinds of phase transitions are outside the scope of this theorem. Such is the case, e.g., of the (Mott) paramagnetic metal - paramagnetic insulator transition. Let us specialize to the case of the triangular lattice.

A. The one-electron DOS

The one-electron DOS is given by

$$N(\omega) = \frac{1}{N} \sum_k A(k, \omega) \quad (15)$$

where N is the number of lattice sites and $A(k, \omega)$, the spectral-weight function, is the imaginary part of the retarded one-electron Green's function.

Mean-field studies at $T=0$ [29] have shown that the half-filled triangular lattice is a paramagnetic metal in the weak-coupling regime, in contrast with the SDW insulating character of the square lattice for small U/t . No gap in the one-electron DOS is, therefore, expected at any temperature for an *infinite* triangular lattice. It has been shown, however, that size effects are very strong in this regime [30]. A gap in the one-electron DOS develops as soon as the spin-spin correlations extend over the whole system. Thus, for lattices of increasing size $N \times N$, the system evolves from a situation where the correlation length $\xi(T) > N$, (with a gap) to one where $\xi(T) < N$ (without a gap). One should be careful when drawing conclusions about the existence of gaps from small lattices.

Fig 4 shows the one-electron DOS of a half-filled 4×4 triangular lattice with periodic boundary conditions. We have taken $U/t = 5$ (\sim half the bandwidth, $9t$), which is a weak to moderate value, and several values of β , $\beta t = 5, 10, 15$ and 20 . Even for βt as high as 20 , the system is far from having a fully developed gap. Since for the bigger lattices one expects weaker pseudogaps, it may be safely concluded that in the weak coupling regime a triangular lattice has no gaps at any temperature, in accordance with the Mermin-Wagner theorem.

In the strong-coupling regime at $T=0$ the system is brought into a commensurate, three-sublattice, 120° twist SDW state (similar to the ground-state of the classical antiferromagnet) which is insulating and stable for increasing U . Quantum fluctuations about the classical antiferromagnetic solution lead to the essential qualitative physics of the Mott-Hubbard insulator at finite temperatures with a charge gap of order U in the spectral-weight function. Fig 5 bears the same information as Fig 4, but with $U/t=20$ which is deep inside the strong-coupling regime. Since size effects are very small in this regime [31], it is fairly clear that a fully developed gap is present at any temperature.

We thus see that, for a given temperature, the system evolves from a gapless situation at small U to a fully developed gap at large U . As U increases through the intermediate-coupling regime, one should find a critical value $U_c(T)$ for which the gap first appears. Fig 6 displays, as Fig 4 and 5, the one-electron DOS for an intermediate value of $U/t=10$ (\sim the bandwidth). As the temperature is lowered from $\beta t = 5$ down to $\beta t = 20$, an incipient pseudogap gradually evolves into a fully developed gap. This value of U is clearly below the critical U for all $\beta t < 20$, i.e., $U_c = 10t$ for $\beta t = 20$. The complementary view is given in Fig 7, which shows the one-electron DOS for $\beta t = 5$ and $U/t = 5, 10, 15$, and 20 . We see the system evolving from a gapless regime to a pseudogap, a deep pseudogap and finally a fully developed gap. Thus $U_c = 20t$ for $\beta t = 5$. In this way one generates a temperature-dependent critical value of the coupling constant $U_c(T)$.

B. The spin structure factor

The spin structure factor, $s(k)$, is given by the k -Fourier transform of the static spin-spin correlation function

$$s_{ij} = \langle \sigma_{iz}(\tau^+) \sigma_{jz}(\tau) \rangle_{\tau=0} \quad (16)$$

where $\tau^+ = \tau + o^+$ in the imaginary-time domain, and $\sigma_{iz} = n_{i\uparrow} - n_{i\downarrow}$.

The peaks of $s(k)$ and corresponding widths in k -space give information, as is well-known, about the SDW's sustained by the system and the spin-spin correlation length. Fig 8 shows $s(k)$ for $\beta t = 20$ and $U/t = 5, 10, \text{ and } 20$, representative values of the three regimes. The almost featureless shape for $U/t = 5$ evolves into two sharp, although small, peaks close to M and M' in the intermediate regime and, finally into a large peak at M' in the strong-coupling regime. The system, correspondingly, evolves from a paramagnetic metal, through an incommensurate spiral SDW, into a Mott-Hubbard insulator

V. CONCLUDING REMARKS

The variation of the one-electron DOS with both temperature and coupling constant seems a useful tool for the purpose of identifying the different regimes of a given system. For the special case of the half-filled repulsive Hubbard model on a triangular lattice, we have identified an intermediate, temperature dependent coupling regime which interpolates smoothly between the weak-coupling (paramagnetic metal) and the strong-coupling (Mott-Hubbard insulator) regimes. As the temperature is lowered in this intermediate-coupling regime, the system evolves from metallic to insulating.

We conclude with a comment on the $\sqrt{3} \times \sqrt{3}$ adlayer structures on group fourth semiconductor surfaces. Although a close connection with the above model study is not claimed, these structures may constitute a physical realization of the three coupling regimes just described, Sn/Ge, Pb/Ge, and SiC being examples of the weak, intermediate and strong coupling regimes, respectively. Despite the added complexity due to electron-phonon interactions and atomic relaxation of both adsorbate and substrate atoms, the model study carried out here provides a general framework for the study of those systems.

Acknowledgments. This work was supported by the DGICYT (Spain) Project N°PB98-0683.

REFERENCES

- [1] G.W. Wannier, Phys Rev **79**, 357 (1950)
- [2] J. Stephenson, J.Math. Phys **5** 1009 (1964)
- [3] P.W. Anderson, Mater. Res. Bull, **8**, 153 (1973)
- [4] H.F. Pen, J.van den Brink, D.I. Khomskii, and G.A. Sawatzky, Phys. Rev. Lett, **78**, 1323 (1997)
- [5] J. M. Campinelli, H.H. Weitering, E.W. Plummer and R. Stumpf, Nature 381, 398 (1996)
- [6] A. Mascaraque, J. Avila, E.G. Michel and M.C. Asensio, Phys. Rev. B. **57** 14758 (1998)
- [7] A. Goldoni, C. Cepek, and S. Modesti, Phys. Rev. B **55**, 4109 (1997).
- [8] J. M. Campinelli, H.H. Weitering, M. Bartkowiak, and E.W. Plummer, Phy. Rev. Lett.**79**, 2859 (1997).
- [9] A. Goldoni, and S. Modesti, Phys. Rev.Lett. **79**, 3266 (1997).
- [10] G. Lelay, V.Y. Aristov, O. Boström, J.M. Layet, M.C. Asensio, J. Avila, V. Huttel, and A.Cricenti, Appl. Surf. Sci.**123-124**, 440, (1998)
- [11] A. Mascaraque, J. Avila, J. Alvarez, M.C. Asensio, S. Ferrer, and E.G. Michel, Phys. Rev. Lett. **82**, 2524 (1999).
- [12] J. Avila, A. Mascaraque, E.G. Michel, M.C. Asensio, J. Ortega, R. Perez, and F. Flores, Phys. Rev. Lett. **82**, 442 (1999)
- [13] H.H. Weitering, J. M. Campinelli, A.V. Malechko, J. Zhang, M. Bartkowiak, and E.W. Plummer, Science **285**, 2107 (1999).
- [14] L.I. Johansson, F. Owman, and P. Martensson, Surf. Sci. **360**, L478 (1998);
J.M. Tremblin, I. Forbeaux, V. Langlais, H. Belkir, and J.M. Debever, Europhys. Lett. **39**, 61 (1997)
- [15] H.H. Weitering, X. Shi, P.D. Johnson, J. Chen, N.J. Dinardo, and S. Kempa, Phys. Rev. Lett. **78**, 1331 (1997).
- [16] K.Würde, P. Krüger, A. Mazur and J. Pollman, Surf. Rev. and Lett. **5**, 105 (1998)
- [17] S. Scandolo, F. Ancilotto, G.I. Chiarotti, G. Santoro, S. Serra and E. Tosatti, Surf. Sci. 402-404, 808 (1998)
- [18] G. Santoro, S. Sorella, F. Becca, S. Scandolo and E. Tosatti, Surf. Sci. 402-404, 802 (1998)
- [19] G. Santoro, S. Scandolo and E. Tosatti, Phys. Rev B **59**, 1891 (1999)
- [20] V.I. Anisimov, A.F. Bedin, M.A. Korotin, G. Santoro, S. Scandolo and E. Tosatti, Phys. Rev B **61**, 1752 (2000)
- [21] R. Blankenbecker, D.J. Scalapino, and R.L. Sugar, Phys Rev. D **24**, 2278 (1981)
- [22] J.E. Hirsch, Phys. Rev B **28**, 4059 (1983)
- [23] J.E. Hirsch, Phys. Rev B **31**, 4403 (1985)
- [24] S.R. White, D.J. Scalapino, R.L. Sugar, E.Y. Loh, J.E. Gubernatis, and R.T. Scalettar, Phys. Rev B **40**, 506 (1989)
- [25] M. Suzuki, Prog Theor.Phys. **56**, 1454 (1976)
- [26] R.N. Silver, D.S. Sivia, and J.E. Gubernatis, Phys. Rev B **41**, 2380 (1990)
- [27] R.N. Silver, J.E. Gubernatis, D.S. Sivia and M. Jarrell, Phys. Rev. Lett. **65**, 496 (1990)
- [28] N.D. Mermin and H. Wagner, Phys Rev. Lett **17** 1133 (1966)

- [29] H.R. Krishnamurthy, C. Jayaprakash, Sanjoy Sarker, and Wolfgang Wenzel, Phys Rev. Lett. **64**, 950 (1990)
- [30] S.R. White, Phys Rev B **46**, 5678 (1992)
- [31] S.R. White, Phys. Rev. B **47**, 1160 (1993)

VI. FIGURE CAPTIONS

Fig 1. Large (outer exagon) and small (inner exagon) surface Brillouin zones (SBZ) of the triangular lattice. Shown are the especial points Γ , M' , K , M , and K' which delimit the contours $\Gamma K M \Gamma$ and $\Gamma M' K' \Gamma$ used in the text.

Fig 2. Band structure of the triangular lattice for $U=0$ in the three-sublattice model. The three bands, ε_k^0 (main band) and ε_k^\pm , are displayed along the $\Gamma K M \Gamma$ contour of the large SBZ in order to show the band crossings and nesting symmetry.

Fig 3. Same as Fig 2, but along the $\Gamma M' K' \Gamma$ contour of the small SBZ.

Fig 4. One-electron density of states (DOS) of the triangular lattice for $U/t=5$ (weak coupling) and decreasing temperature, $\beta t=5, 10, 15$, and 20

Fig 5. Same as Fig 4, but for $U/t=20$ (strong coupling).

Fig 6. Same as Figs 4 and 5, but for $U/t=10$ (intermediate coupling).

Fig 7. One-electron DOS of the triangular lattice for increasing $U/t=5, 10, 15$, and 20 at a fixed temperature $\beta t=5$.

Fig 8. Low-temperature ($\beta t=20$) spin structure factor, $s(k)$, of the triangular lattice in the weak ($U/t=5$), intermediate ($U/t=10$) and strong ($U/t=20$) coupling regimes

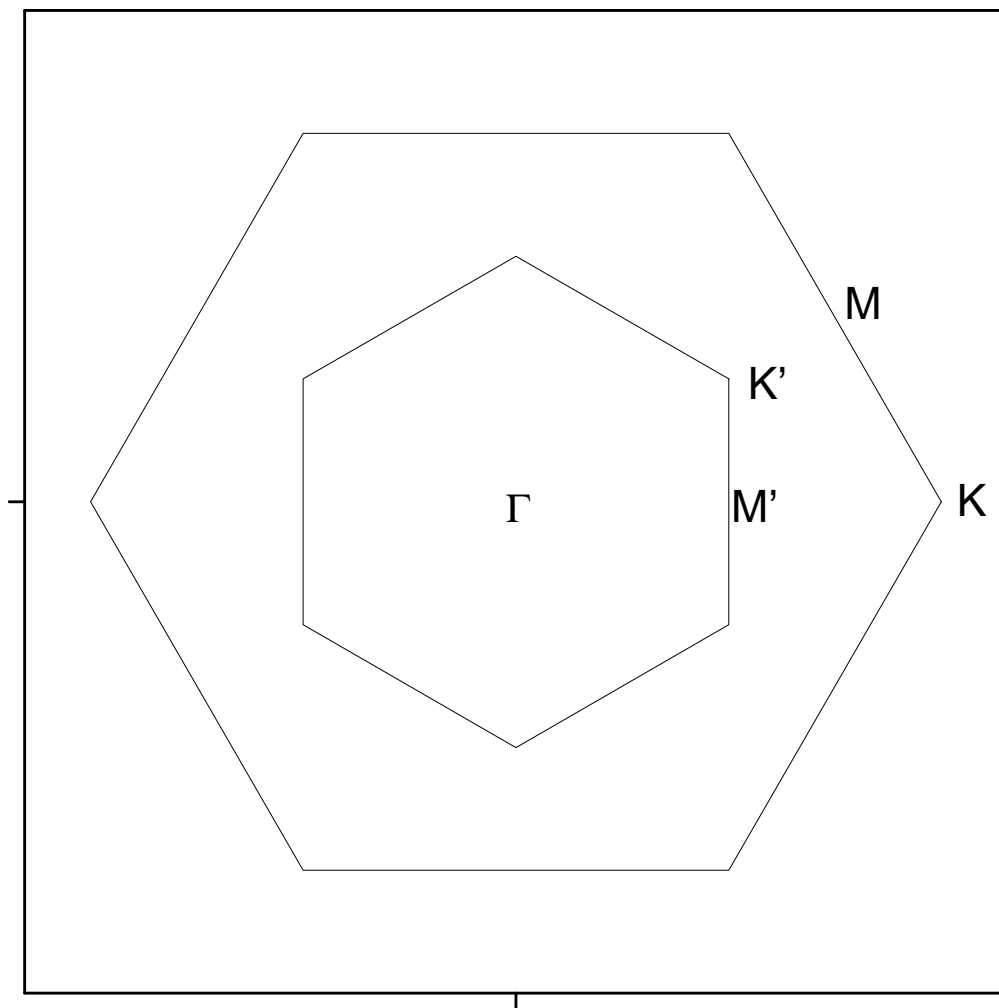


Fig 1

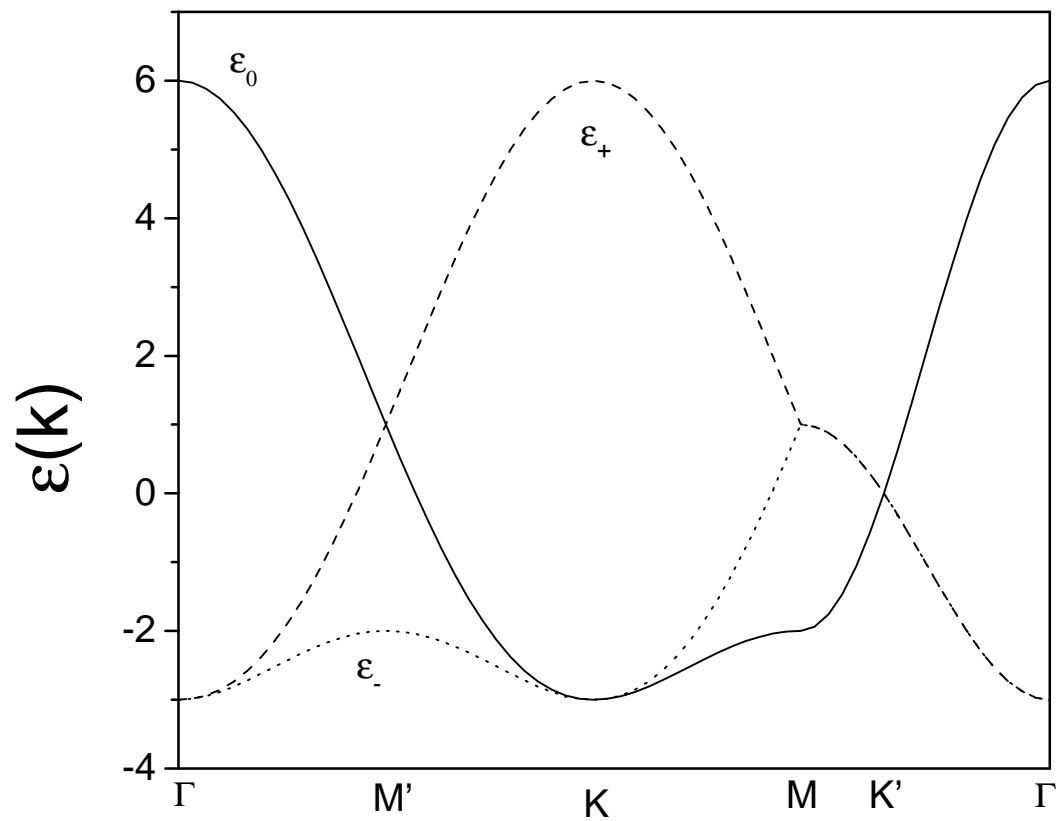


Fig 2

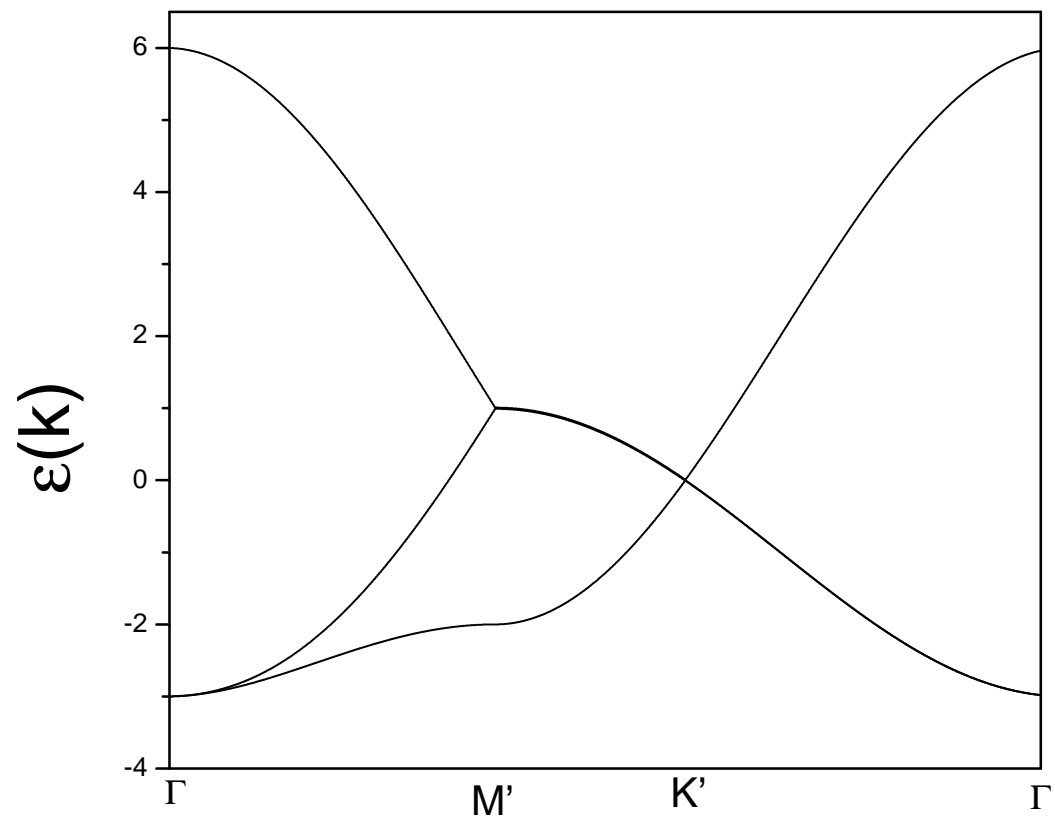


Fig 3

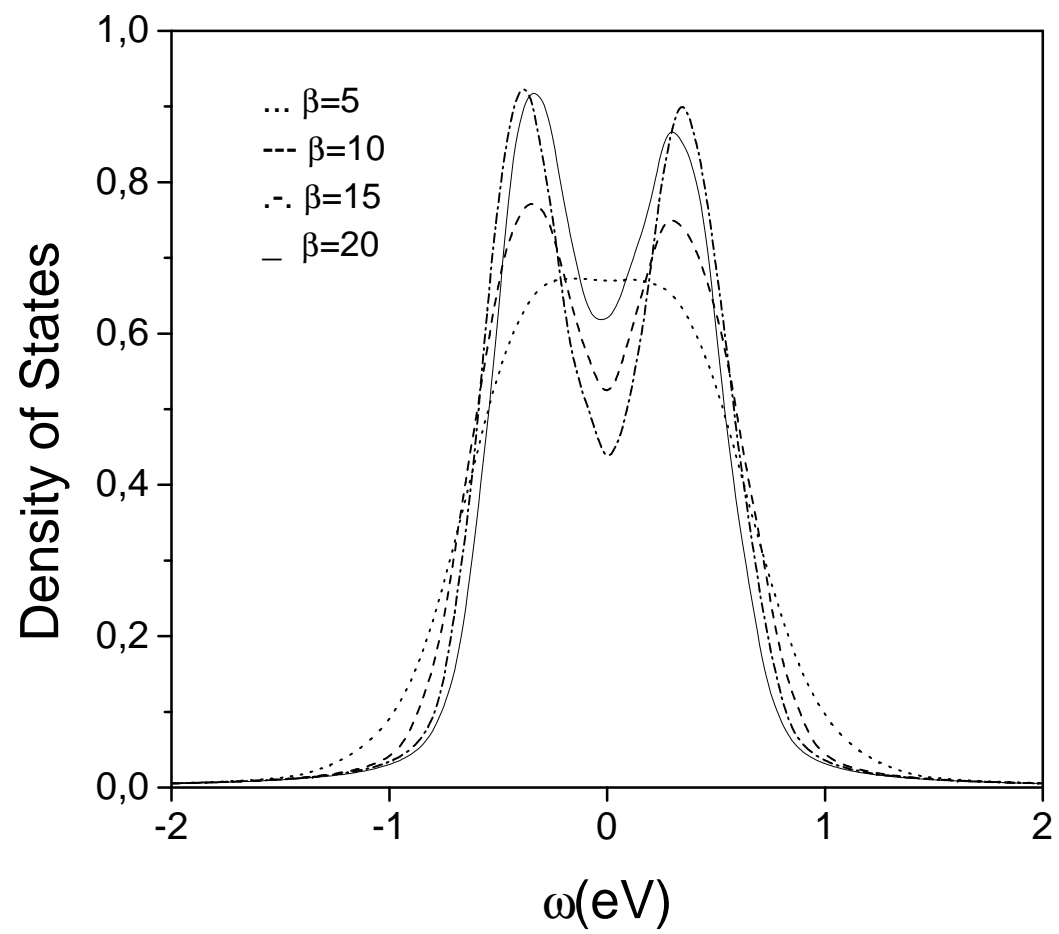


Fig 4

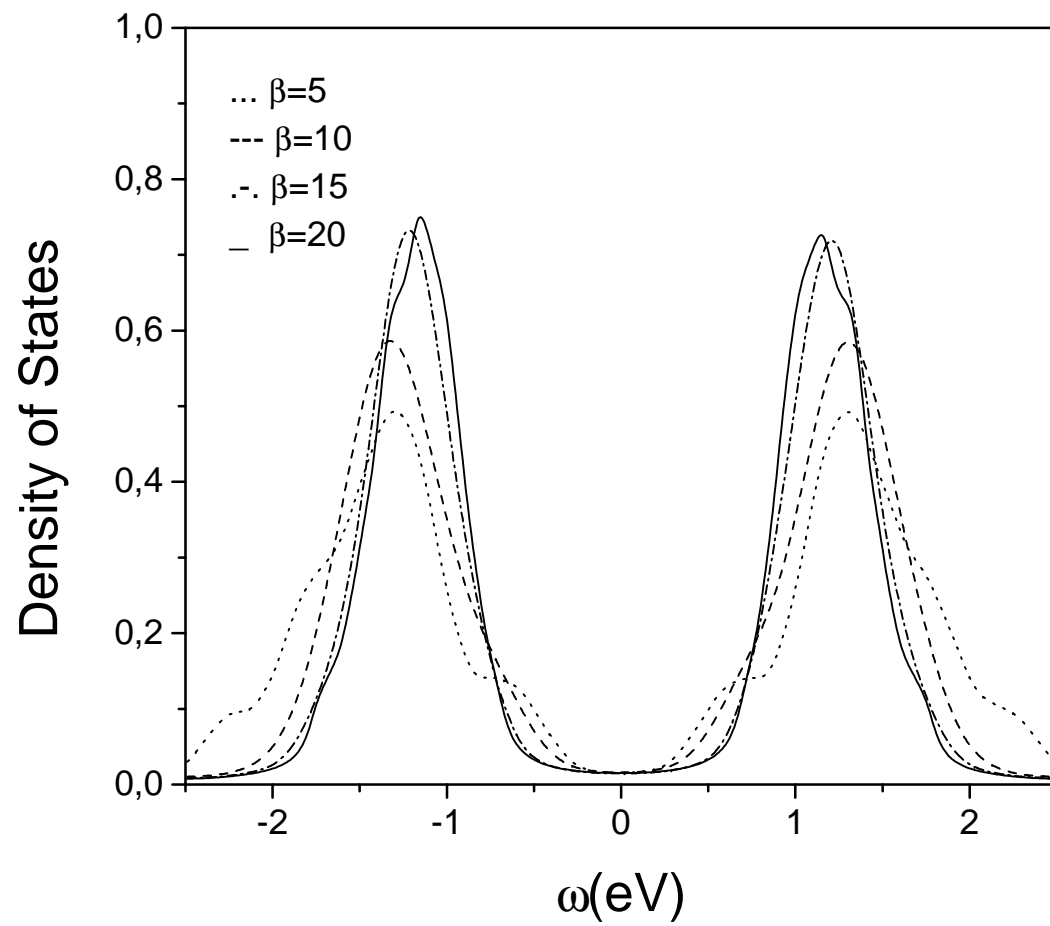


Fig 5

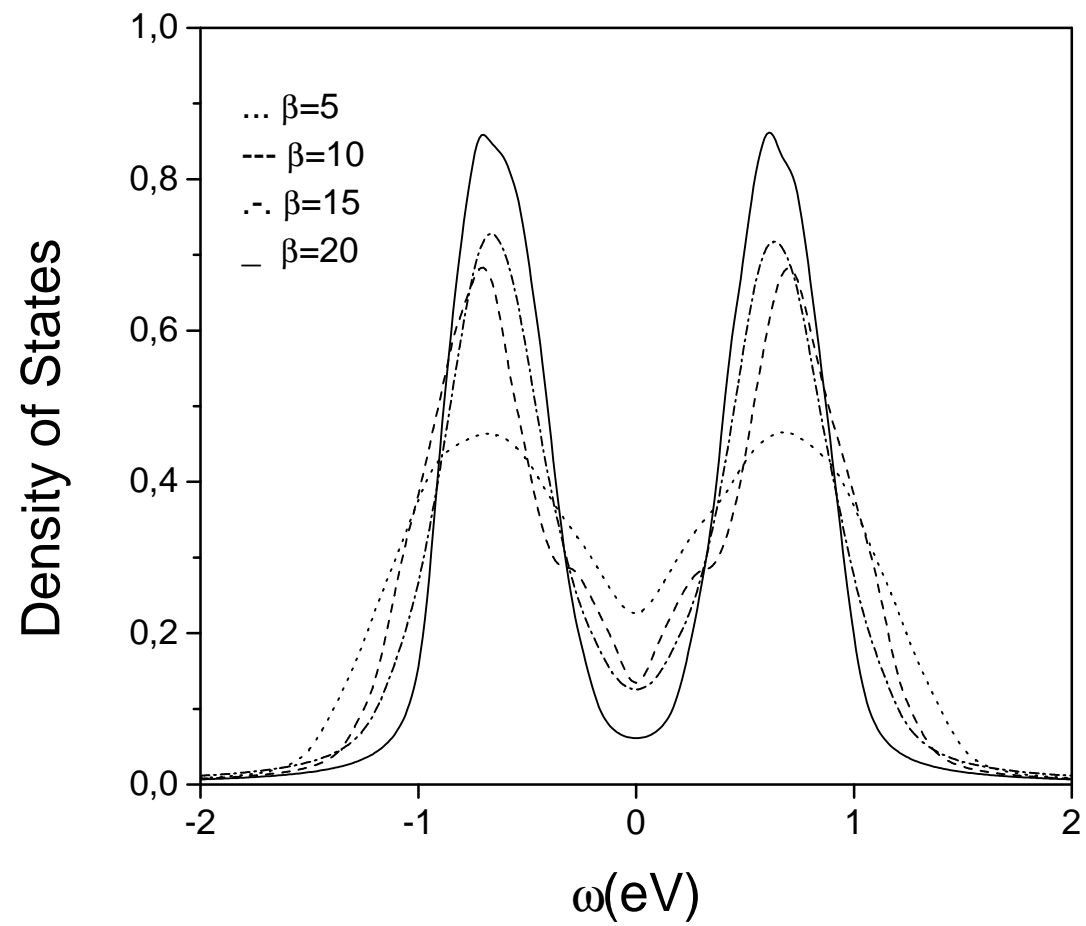


Fig 6

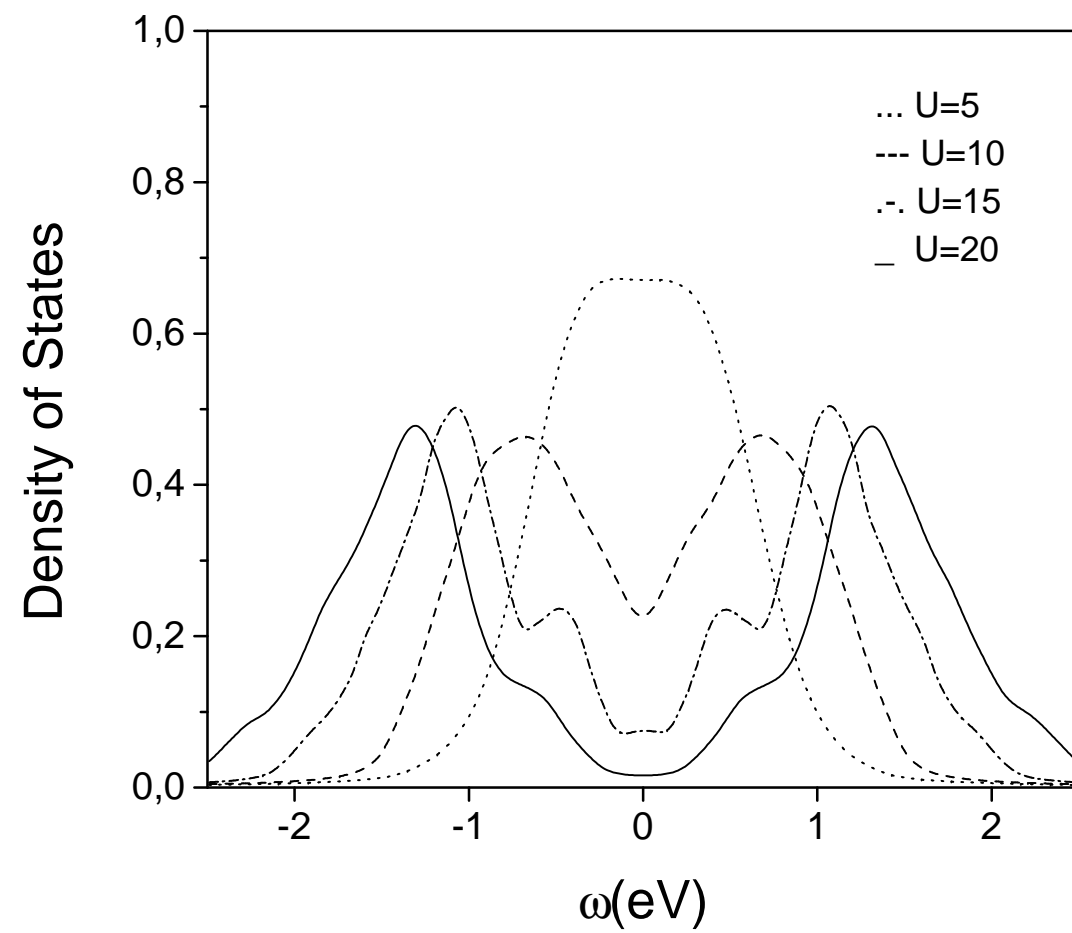


Fig 7

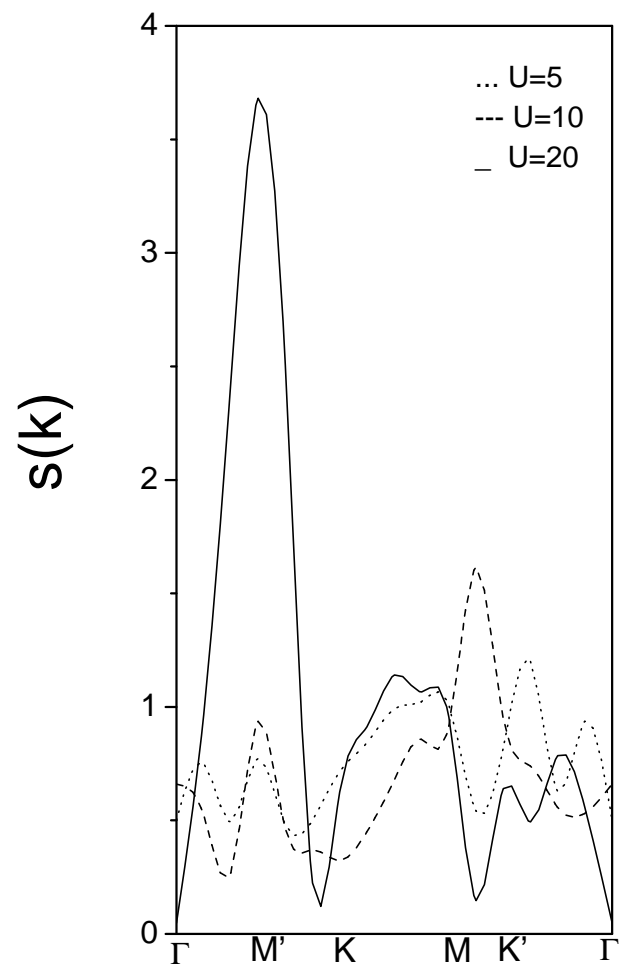


Fig 8